

Triple tracks in CR-39 as the result of Pd–D Co-deposition: evidence of energetic neutrons

Pamela A. Mosier-Boss · Stanislaw Szpak ·
Frank E. Gordon · Lawrence P. G. Forsley

Received: 30 July 2008 / Revised: 3 September 2008 / Accepted: 14 September 2008 / Published online: 1 October 2008
© Springer-Verlag 2008

Abstract Since the announcement by Fleischmann and Pons that the excess enthalpy generated in the negatively polarized Pd–D–D₂O system was attributable to nuclear reactions occurring inside the Pd lattice, there have been reports of other manifestations of nuclear activities in this system. In particular, there have been reports of tritium and helium-4 production; emission of energetic particles, gamma or X-rays, and neutrons; as well as the transmutation of elements. In this communication, the results of Pd–D co-deposition experiments conducted with the cathode in close contact with CR-39, a solid-state nuclear etch detector, are reported. Among the solitary tracks due to individual energetic particles, triple tracks are observed. Microscopic examination of the bottom of the triple track pit shows that the three lobes of the track are splitting apart from a center point. The presence of three α -particle tracks outgoing from a single point is diagnostic of the $^{12}\text{C}(\text{n},\text{n}')3\alpha$ carbon breakup reaction and suggests that DT reactions that produce ≥ 9.6 MeV neutrons are occurring inside the Pd lattice. To our knowledge, this is the first report of the production of energetic (≥ 9.6 MeV) neutrons in the Pd–D system.

Keywords CR-39 · Palladium · Neutrons

Introduction

CR-39 is an allyl glycol carbonate plastic that has been widely used as a solid-state nuclear track detector. These detectors have been used extensively to detect and identify such fusion products as p, D, T, ^3He , and α particles resulting from inertial confinement fusion (ICF) experiments (Séguin et al. 2003). They have also been used to detect neutrons (Phillips et al. 2006). When a charged particle passes through the CR-39 detector, it leaves a trail of damage along its track inside the plastic in the form of broken molecular chains and free radicals (Frenje et al. 2002). After treatment with an etching agent, tracks remain as holes or pits. The size and shape of these pits provide information about the mass, charge, energy, and direction of motion of the particles (Nikezic and Yu 2004). Therefore, CR-39 detectors can semiquantitatively be used to distinguish the types and energies of individual particles. Advantages of CR-39 for ICF experiments include its insensitivity to electromagnetic noise; its resistance to mechanical damage; and its relative insensitivity to electrons, X-rays, and γ -rays. Consequently, CR-39 detectors can be placed close to the source without being damaged. Furthermore CR-39, like photographic film, is an example of a constantly integrating detector, which means that events are permanently stamped on the surface of the detector. As a result, CR-39 detectors can be used to detect events that occur either sporadically or at low fluxes.

Earlier, the use of CR-39 to detect the emission of energetic particles resulting from Pd–D electrolysis

Electronic supplementary material The online version of this article (doi:10.1007/s00114-008-0449-x) contains supplementary material, which is available to authorized users.

P. A. Mosier-Boss (✉) · S. Szpak · F. E. Gordon
SPAWAR Systems Center Pacific,
Code 7173,
San Diego, CA 92152, USA
e-mail: pam.boss@navy.mil

L. P. G. Forsley
JWK International Corp.,
Annandale, VA 22003, USA

experiments has been demonstrated (Oriani and Fisher 2002, Lipson et al. 2000). In the experiments conducted by Oriani and Fisher (2002), the CR-39 detectors were placed above and below the Pd foil cathode so as to not impede uniform loading of the cathode with deuterium. Although this experimental geometry is not optimum, they were still able to detect charged particles significantly above background. Lipson et al. (2000) prepared Au/Pd/PdO heterostructures that were electrochemically loaded with deuterium. After electrolysis, the Au/Pd/PdO heterostructure was placed in contact with CR-39, and tracks consistent for 2.5–3.0 MeV protons and 0.5–1.5 MeV tritons were measured. More recently, experiments with CR-39 detectors have been performed using the Pd–D co-deposition process (Szpak et al. 2007). After etching, it has been observed that the density of tracks on the CR-39 detector is greatest where the cathode had been in contact with the detector (Mosier-Boss et al. 2007). This indicates that the source of the tracks is the Pd that had been plated on the cathode. The distribution of the tracks along the length of the cathode is inhomogeneous suggesting that some Pd sites are more active than others. Results of these experiments also showed that the production of charged particles occurred in bursts. Control experiments indicated that the tracks were not due to radioactive contamination of the cell components; nor were they due to impingement of D₂ bubbles on the surface of the CR-39 detector; nor were they the result of chemical attack by D₂, O₂, or Cl₂ (Mosier-Boss et al. 2007). These experiments also indicated that LiCl is not essential for the production of energetic particles and that the density of tracks significantly decreases, by at least three orders of magnitude, when H₂O is substituted for D₂O. Since the natural abundance of deuterium in light water is 0.015%, it is possible that the tracks observed in the light water experiments could actually be due to Pd–D interactions. Microscopic examination of the CR-39 detectors used in Pd–D electrolysis has been done in areas where the density of tracks is less. In these areas, what appear to be triple tracks are observed interspersed among the solitary tracks. The number of these triple tracks is very low—on the order of a ten or less per detector and are only observed in heavy water experiments. These triple tracks have been observed in every Pd–D co-deposition experiment that has been conducted using Ag, Au, or Pt cathodes in both the presence and absence of an external electric or magnetic field. When Ni screen is used as the cathode, tracks and triple tracks are only observed when an external electric or magnetic field is applied. Triple tracks are indicative of a reaction resulting in the formation of three particles of equal mass and energy. In this communication, the origins of these triple tracks are investigated.

Materials and methods

Details on cell design and operation have been described elsewhere (Mosier-Boss et al. 2007). In these particular experiments, Pd was plated out from a 0.03-M PdCl₂, 0.3-M LiCl solution in D₂O or H₂O onto either a Ni, Ag, Au, or Pt cathode that was in contact with a CR-39 detector. In some experiments, a 60- μ m thick polyethylene film was placed between the cathode and the CR-39 detector. Upon completion of the experiment, which typically run 2–3 weeks, the cathode was disassembled and the CR-39 detector was etched in 6.5 M NaOH. Etching conditions are indicated in the figure captions. The CR-39 detector was then subjected to microscopic examination using an Eclipse E600 epifluorescent microscope (Nikon), and images were taken using a CoolSnap HQ CCD camera (Photometrics). The front and back surfaces of the CR-39 detectors were also analyzed using an automated scanning system to obtain quantitative information on the tracks.

Results

Figure 1a and b show images obtained for a CR-39 detector that had been exposed to an ²⁴¹Am source that emits 5.5 MeV α particles. The tracks are conical in shape (Yoshioka et al. 2005). When viewed through a microscope and focusing on the surface of the CR-39 detector, the pits are symmetrical and dark in color (top images in Fig. 1a and b). The pits can be either circular in shape or elliptical. Circular pits result from particles that have entered the surface at a normal incidence while elliptical pits result from particles entering the surface at an angle. When focusing deeper into the CR-39 detector, bright points of light are observed in the center of the pits (bottom images in Fig. 1a and b). These bright points are due to the bottom tip of the conical track. When backlit, the bottom tip of the track acts like a lens and appears as a bright spot inside the track.

Pits very similar to the ones shown in Fig. 1a have been observed for CR-39 detectors that have been subjected to a Pd–D co-deposition experiment (Szpak et al. 2007; Mosier-Boss et al. 2007). Specifically, the pits are dark in shape and show bright spots inside when focusing deeper inside the pit. It should be noted that tracks have been observed on the backside of the 1-mm thick CR-39 detectors. The origins of these tracks are still under investigation. However, preliminary data and discussion of these tracks is provided in S1 (Electronic supplementary material). Where the density of tracks is less, triple tracks are observed interspersed among the solitary tracks, as shown in Fig. 1c. Examples of these triple tracks at higher magnification are shown in Figs. 1d and 2. Possible

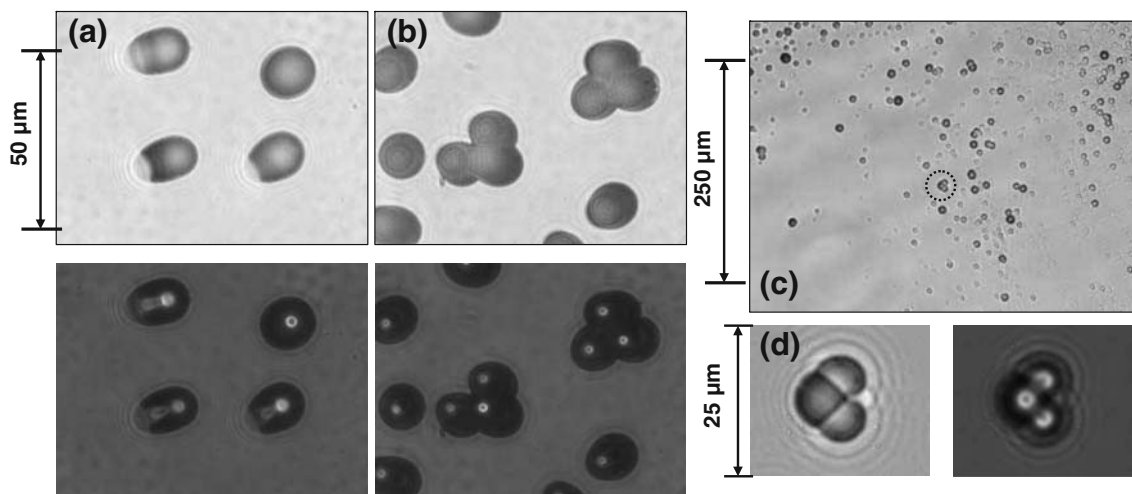


Fig. 1 **a, b** Images of pits in CR-39 created by exposure to an ^{241}Am source, $\times 1,000$ magnification. The CR-39 detector had been etched for 12 h in 6.5 M NaOH at 62°C . The *top photomicrographs* were taken with the focus on the surface of the CR-39 detector. The bottom photomicrographs are an overlay of two images taken at two different focal lengths (*surface and bottom of the pits*). **c** Image of a triple track

(*circled*) among the solitary tracks (magnification $\times 200$). The CR-39 detector had been etched for 6 h in 6.5 M NaOH at 62°C . **d** Image of the triple track shown in (c) at magnification $\times 1,000$. In the *left image*, the focus is on the surface of the CR-39 detector while the image on the *right* is an overlay of two images taken at two different focal lengths (*surface and bottom of the pits*)

explanations for the formation of a triple track are (1) that it is due to overlapping single tracks or (2) it is the result of reactions that emit three particles of similar mass and energy. Figure 1b shows triple tracks resulting from overlapping tracks due to the α particles emitted from an ^{241}Am source. The microscope was focused on the bottom of these triple tracks. The image, Fig. 1b bottom microphotograph, shows that each lobe of the triple track has a distinct separate bright spot. This contrasts with triple tracks obtained as the result of a Pd–D co-deposition experiment. Focusing inside the bottom of the triple track pit, Fig. 1d right image and Fig. 2a, b right images, it appears that the individual lobes of the triple track are splitting apart from a center point. This favors explanation (2) as the source of these triple pits. The number of triple tracks observed in these CR-39 detectors is very low. It is estimated that less than ten such tracks are present on each detector. They have been observed on both the front and back sides of the CR-39 detector. There are probably more such triple tracks present in the regions where the density of pits is higher. However, differentiating them from overlapping pits is difficult.

The CR-39 detectors have been immersed in the electrolyte, and they have been placed in contact with the wires and screens used as cathode materials (Mosier-Boss et al. 2007). After etching, a few solitary tracks were observed randomly distributed in the CR-39 detectors. No triple tracks were observed. These results indicate that the tracks observed in the CR-39 after a Pd–D co-deposition experiment are not due to radioactive contamination of the

cell components or to some chance exposure to a DT neutron source. Additional control experiments have been conducted that indicate that the triple tracks shown in Figs. 1d and 2a,b do not have a chemical origin. No tracks were observed when electrolysis in deuterated water was done using Ag wire or Ni screen in place of the Pd–D co-deposition (Mosier-Boss et al. 2007). Experiments were conducted by replacing PdCl₂ with CuCl₂ (Mosier-Boss et al. 2007). In these experiments, the electrochemical reactions occurring for both the PdCl₂ and CuCl₂ systems are the same. At the cathode, the metal plates are out in the presence of evolving D₂ gas while, at the anode, O₂ and Cl₂ evolution occurs. The only difference is that metallic palladium absorbs deuterium and copper does not. While tracks, including triple tracks, are observed in the Pd–D system, no tracks are observed in the Cu–D system. Experiments have also been conducted in which a 60- μm thick polyethylene film has been placed between the cathode used in Pd–D co-deposition and the CR-39 detector. When these detectors were etched, tracks, including the triple tracks shown in Fig. 2b, are observed. Besides neutrons, linear energy transfer (LET) curves indicate that >2 MeV protons and >10 MeV α can penetrate 60 μm of polyethylene. If the triple tracks were due to structure defects, they would have been observed in the control experiments. Since no triple tracks were observed in the control experiments, the triple tracks resulting from Pd–D co-deposition cannot be attributed to defects in the structure of the CR-39 detectors. Both the Cu–D co-deposition experiments (Mosier-Boss et al.

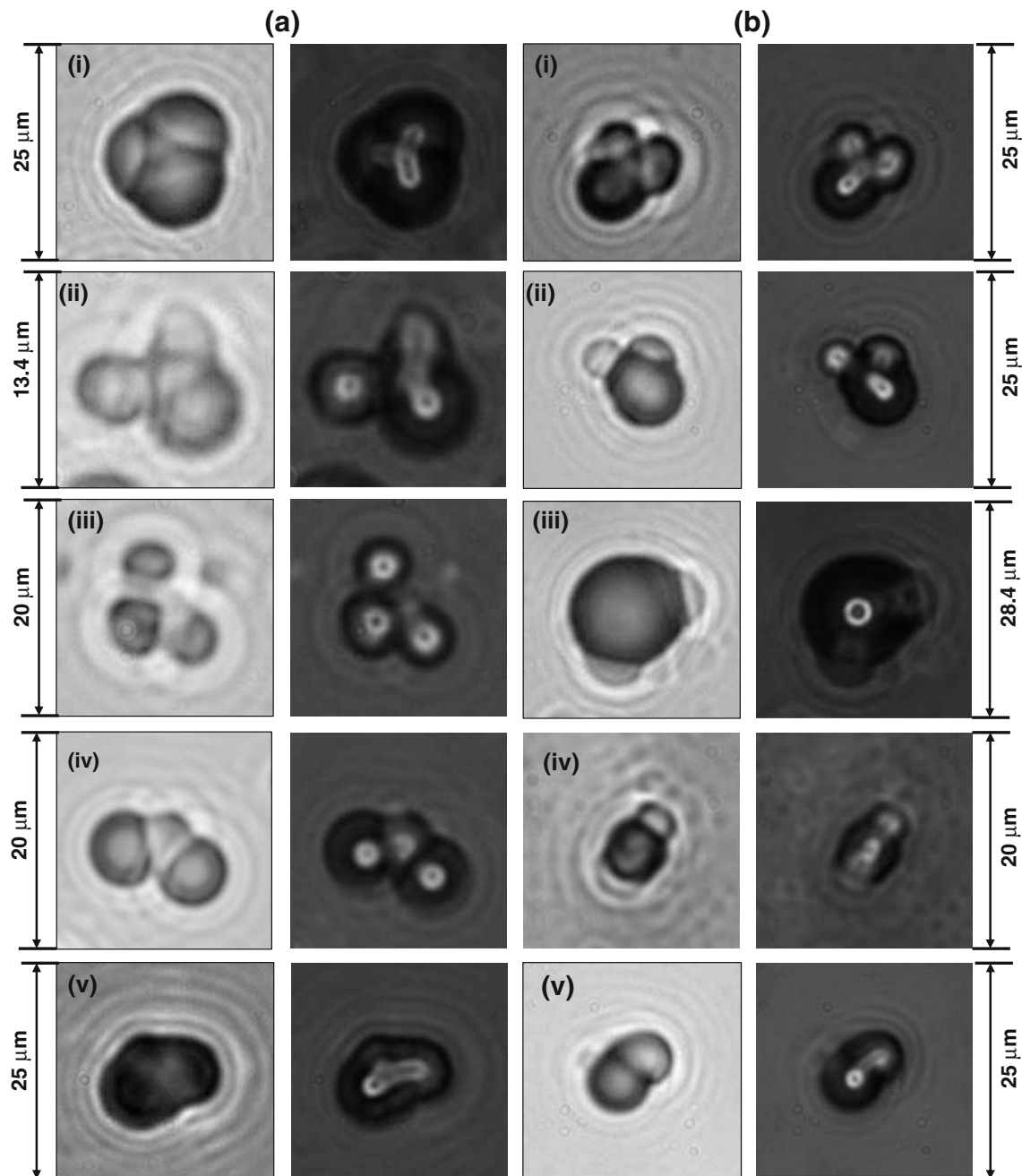


Fig. 2 Images (magnification $\times 1,000$) of triple tracks observed in CR-39 detectors subjected to a Pd–D co-deposition experiment. The CR-39 detector has been etched in 6.5 M NaOH at 62°C. **a** Experiments conducted with the cathode in direct contact with the CR-39 detector. For image *i*, the detector was etched for 10 h while for images *ii–v*, the detectors were etched for 6 h. **b** Experiments conducted with a 60- μm

thick polyethylene film between the cathode and the CR-39 detector. For images *i* and *v*, the detectors were etched for 6 h and for images *ii–iv*, the detectors were etched for 10 h. For both **(a)** and **(b)**, the *left images* were obtained with the focus on the surface of the CR-39 detector while the images on the *right* are an overlay of two images taken at two different focal lengths (*surface and bottom of the pits*)

2007) and the experiments with the 60- μm polyethylene film between the cathode and CR-39 detector, summarized in Fig. 2b, indicate that the triple tracks cannot be attributed to the metal dendrites piercing into the CR-39 or to localized production of hydroxide ions that etch into the CR-39.

Discussion

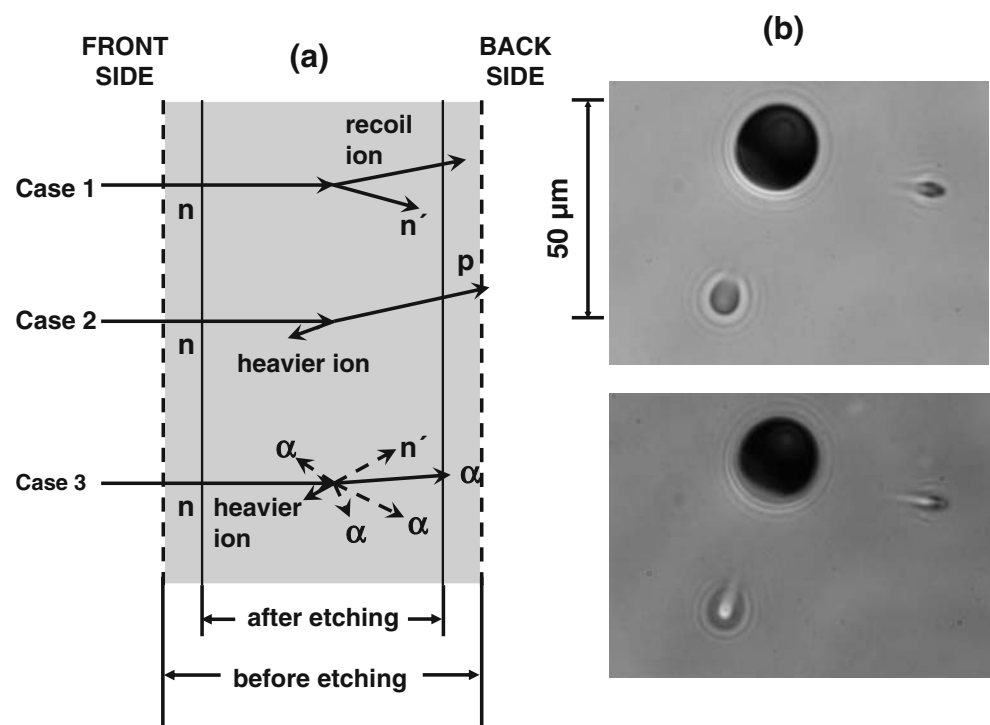
Besides being used to detect energetic particles, CR-39 has also been used to measure neutron yields from DD and DT implosions (Frenje et al. 2002). The possible interactions of

DD neutrons (2.45 MeV) and DT neutrons (14.1 MeV) are described in Fig. 3a. In the interaction shown in case 1, the DD and DT neutrons can scatter elastically, producing recoil protons, carbons, or oxygen nuclei in the forward direction. But, DT neutrons can also undergo two inelastic (n,p and n,α) reactions with carbon or oxygen, case 2 and case 3, respectively in Fig. 3a. These inelastic reactions result in charged particles that can produce tracks on the front and/or the back side of the CR-39 detector. As indicated in Fig. 3a, knock-on tracks resulting from fast neutrons should appear uniformly throughout the CR-39 detector which would be revealed by sequential etching of the detectors. As the CR-39 detector is etched longer, the tracks on the surface of the detector become larger in size and shallower. However, longer etching of the detectors reveals additional tracks deeper inside the detector (Fig. 3b). In Fig. 3b, a circular pit was first observed on the surface after a 6-h etch of the detector. After additional etching, two new tracks are observed—one below and one to the right of the large circular track.

As illustrated in Fig. 3a, the case 3 interaction includes both the (n,α) reaction (solid arrows) and the carbon breakup reaction (dashed arrows). The main constituent of CR-39 is ^{12}C (32% by weight), which can be used as both a target and a detector for energetic neutrons (Antolković and Dolenc 1975). In the carbon breakup reaction, a metastable ^{13}C shatters into three α particles and the residuals of the reaction can be viewed in the CR-39 detector as a three-prong star where each prong represents

each charged particle that occurs in the decay (Antolković and Dolenc 1975). There are varying reports on the energy required to shatter a carbon atom. Al-Najjar et al. (1986) reported that the threshold energy of the neutron required to shatter a carbon atom to form a three-prong star is 9.6 MeV. Aframian (1983) reported that triple tracks of $^{12}\text{C}(n,n')3\alpha$ were clearly visible in the detectors when exposed to 10.7 MeV neutrons. Abdel-Moneim and Abdel-Naby (2003) estimated the energy of the incident neutrons needed to create triple tracks by measuring the length, depth, and space direction of the three-prong α tracks. From these data, they were able to compute the triple- α momentum configuration. From these calculations, they estimated the neutron energy to be 14.3 ± 1.6 MeV. Photomicrographs of the three prong stars reported by Al-Najjar et al. (1986), Abdel-Moneim and Abdel-Naby (2003), Palfalvi et al. (2005), and Sajó-Bohus et al. (2005) are similar to those shown in Figs. 1d and 2. Palfalvi et al. (2005) have obtained photomicrographs in which the focus is inside the triple track. In these photomicrographs, it can be seen that the lobes of the triple track are splitting apart from a center point. Palfalvi et al. (2005) photomicrographs of the inside of the triple track resemble those shown in the right images in Figs. 1d, 2a and b. Instead of separate distinct bright spots as observed for the overlapping ^{241}Am α tracks in Fig. 1b bottom image, the triple tracks resulting from Pd–D co-deposition show three α tracks outgoing from a single point (Figs. 1d, 2a, and b right images).

Fig. 3 **a** Schematic drawing of the CR-39 track detector and the neutron interaction processes that can take place inside the plastic (Frenje et al. 2002). The drawing is not to scale. *Case 1* summarizes the DD neutrons interaction with CR-39. *Cases 1–3* describe the DT neutron interactions with CR-39. **b** Images of a CR-39 detector taken after the detector has been etched for 60 h 6.5 M NaOH at 62°C. The detector is 106 μm thinner (53 μm have been removed from both sides of the detector). *Top image* was taken with the focus on the surface of the detector. The *bottom image* is an overlay of two images taken at two different focal lengths (*surface and bottom of the pits*)



The presence of three α -particle tracks outgoing from a single point is diagnostic of the $^{12}\text{C}(n,n')3\alpha$ carbon breakup reaction and is easily differentiated from other neutron interactions occurring within the CR-39 detector (Durrani and Bull 1987; Al-Najjar et al. 1986; Abdel-Moneim and Abdel-Naby 2003; Pálfalvi et al. 2005; Sajó-Bohus et al. 2005). Consequently, analysis of the CR-39 detectors used in the Pd–D co-deposition experiments has concentrated on looking for these three prong stars as their identification is unambiguous. Although the three α particles resulting from the $^{12}\text{C}(n,n')3\alpha$ carbon breakup reaction can completely fly apart, as has been observed for CR-39 detectors exposed to DT generators, such particles would be difficult to differentiate from tracks that result from three separate solitary events. This is especially true given the density of tracks (Fig. 1c) observed in the Pd–D co-deposition experiments using the current protocol (Mosier-Boss et al. 2007). However, Fig. 2a, ii shows a triple track in which one track is separated from the other two tracks, and Fig. 2a, iii shows a triple track that has all three tracks separated from one another. The relative size of the triple tracks (Fig. 2) to one another is not relevant. The $^{12}\text{C}(n,n')3\alpha$ carbon breakup reaction can occur anywhere on the surface or inside the CR-39 detector. After etching, triple tracks generated closer to the surface of the CR-39 detector will appear larger than those created deeper inside the detector.

The $^{12}\text{C}(n,n')3\alpha$ reaction is anisotropic (Abdel-Moneim and Abdel-Naby 2003). Likewise, the reactions producing the triple tracks during Pd–D co-deposition should be anisotropic. This anisotropy is illustrated by comparing the images in Fig. 2a, i, ii and b, i–iii with those in Fig. 2a iii–v and b, v. In the images shown in Fig. 2a, i, ii and b, i–iii, the α particles are approximately in the same plane as the center point. However, in the images shown in Fig. 2a, iii–v and b, v, it can be seen that, as the carbon atom has been shattered, one α particle has been shot below the plane of the center point and two α particles have been ejected above the plane of the center point.

Knowing the threshold energy needed to shatter a carbon atom and the distance each α particle of the triple track has traversed in the CR-39, the energy of the neutron that created that triple track can be estimated. LET curves are used to determine the stopping distance of alphas in CR-39 as a function of α particle energy. These LET curves were calculated using the SRIM-2003.26 code of Ziegler and Biersack (1985). In the photomicrographs shown in Fig. 2a, i, ii and b, i, the distance between the center point and one of the prongs of the triple track vary between 4.41 and 4.60 μm . Using the LET curves for CR-39, the energy of the α particles are between 1.0 and 1.1 MeV. This is the energy carried away by each α particle after the carbon atom was shattered by an energetic neutron. The threshold

energy to shatter a carbon atom is 9.6 MeV (Al-Najjar et al. 1986). The energy of the neutrons that generated the tracks shown in Fig. 2a, i, ii and b, i is estimated to be between 12.6 and 12.9 MeV. The photomicrograph shown in Fig. 2b, iii indicates that two alphas are carrying off the excess energy after the carbon has shattered. The distance between the center point and the prongs of the triple track is 13.65 μm . The LET curves for CR-39 indicate that the energy of the alphas is 2.92 MeV. The energy of the neutron that generated this triple track is estimated to be 15.44 MeV.

There have been reports of neutron emissions in the Pd–D system (Jones et al. 1989; Takahashi et al. 1990; Lipson et al. 2000; Mizuno et al. 2001). To our knowledge, this is the first report of the evidence of the emission of ≥ 9.6 MeV neutrons formed in situ during a Pd–D electrolysis experiment. Further work is required to determine the reaction(s) that give rise to these energetic neutrons. At this time, however, two possible sources of these neutrons can be considered. One is secondary DT fusion reactions involving energetic tritons produced from primary DD fusion reactions (Phillips et al. 1998). The other is multibody fusion reactions involving deuteria “clusters” inside a metal lattice (Takahashi 1994).

The data that support DT fusion for the production of energetic neutrons in Pd–D co-deposition are: (1) neutrons produced by DT fusion have energies ranging between 11.9 and 17.2 MeV (Phillips et al. 1998). Using LET curves, the estimated neutron energies that generated the triple tracks in CR-39 used in the Pd–D co-deposition experiments fall in this range; (2) the tracks attributed to the three α reactions as determined from the automated scanned results of the backside of the CR-39 are in agreement with the manually observed number of triple tracks (see “[Electronic supplementary material](#)” for further discussion); (3) the observation of p–T double tracks in CR-39 (Lipson et al. 2000); and (4) reports of tritium production, using liquid scintillation techniques, in electrolytic Pd–D cells (Packham et al. 1989; Chien et al. 1992) as well as in Pd–D co-deposition (Szpak et al. 1998). Unfortunately, the liquid scintillation technique cannot differentiate an increase in tritium concentration due to electrolytic enrichment from generation as the result of DD fusion. One approach to differentiate both sources of tritium is to show that the observed increase in tritium correlates with the production of 3.0 MeV protons. This has been demonstrated by both Lipson et al. (2000) and Jones et al. (1990). Tritium generated as the result of DD reactions should have an energy of 1.01 MeV (Srinivasan 1991). However, this is the energy of tritons that have been created in a plasma. In the Pd–D co-deposition experiments, the cathode is immersed in deuterated water and, as discussed in “[Electronic supplementary material](#)”, the presence of water will slow down the emitted particles.

As long as the triton is not completely thermalized, it will undergo DT fusion to form a 14.1-MeV neutron. The p-T double tracks in CR-39 reported by Lipson et al. (2000) indicate that these tritons are energetic, and the cross section of DT fusion is higher than that of DD fusion (Lawson 1957). Analysis of the tracks present on the backside of the CR-39 detector (see “[Electronic supplementary material](#)” for further discussion) show that the observed size distribution exhibits features that are consistent with both DD and DT fusion reactions.

The multibody reactions proposed by Takahashi (1994) involve deuteria occupying the tetrahedral and octahedral sites in the metal lattice. In the proposed 3D and 4D fusion reactions occurring in the metal deuterides, high-energy α particles are formed that dissociate deuterons in the system to produce neutrons with a continuous spectrum in the 0 to 10 MeV region. These high energy α particles are also expected to produce Bremsstrahlung X-rays. Experimental data that support this mechanism are evidence of recoil carbon and oxygen atoms on the backside of the CR-39 suggestive of 1.25–8 MeV neutrons (see discussion in “[Electronic supplementary material](#)”) and Bremsstrahlung radiation that has been observed in the X-ray and γ -ray spectra obtained during Pd–D co-deposition (Szpak et al. 1996).

Measuring the emission of energetic neutrons is challenging. In order to be detected using ^{10}B , ^6Li , or ^3He detectors, the neutron needs to be thermalized. This requires placing hydrogen-rich materials between the neutron source and the detector, which will impact the collection efficiency of the detector. In addition, when using electronic-based detectors, long acquisition times are typically used to improve the signal to noise ratio (S/N). However, if the rate of production is sporadic and/or at a low level, the signal can be averaged away. As discussed *vide supra*, this is not a limitation for CR-39 detectors. Furthermore, the energetic α , p, T, and ^3He species formed as the result of DD and DT fusion should also leave tracks in the CR-39 (Frenje et al. 2002). In principle, one would expect that the statistics of these interactions could be deduced by analyzing the tracks on the side of the CR-39 detectors that had been in contact with the cathode. However, differentiating these species using the CR-39 track data can be difficult. The size and shape of the tracks formed in the CR-39 detectors depend upon the energy, charge, and mass of the emitted particle as well as the angle of incidence. Calibration of the CR-39 detectors is done by either exposing the detectors to sources emitting particles of known energy or by placing them in accelerators used to generate charged particles. Even under ideal conditions, there is significant overlap in the track sizes of the different particles. In the Pd–D co-deposition experiments, the particles that are emitted have to traverse through a thin

film of heavy water before reaching the detector surface. This will slow the particles down, which will further complicate speciation. Calibration efforts are currently underway. However, the effect of water on the energetics of the particles and on the size distribution of the tracks is discussed in more detail in “[Electronic supplementary material](#)”. In order to say anything conclusive about reaction rates, the reactions need to occur at a constant rate. That is not true of the Pd–D system. Events that produce heat (Szpak et al. 2004), γ and/or X-ray radiation (Szpak et al. 1996), tritium (Szpak et al. 1998), and energetic particles (Szpak et al. 2007) in cathodes produced by Pd–D co-deposition occur sporadically and in bursts.

The mechanism by which DD and DT fusion reactions can occur in Pd is not yet understood; nevertheless, theories are currently under development. However, since no tracks, single or triple, were obtained when CuCl_2 was used in place of PdCl_2 , it can be concluded that the deuterium must be inside a metal lattice for these reactions to occur and not simply adsorbed on the surface of the metal. This implies that the metal lattice facilitates these reactions indicating that nuclear phenomena can be influenced by the atomic and electronic environment.

Acknowledgement This work was funded by the SSC-Pacific ILIR program and JWK Corporation. The authors would like to thank Dr. Gary Phillips, nuclear physicist, retired Naval Research Laboratory, US Navy, Radiation Effects Branch, and Dr. Roger Boss of SSC-Pacific for valuable discussions in interpreting the data.

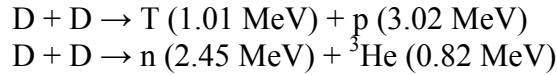
References

- Abdel-Moneim AM, Abdel-Naby A (2003) A study of fast neutron beam geometry and energy distribution using triple- α reactions. *Radiat Meas* 37:15–19
- Aframian A (1983) Disintegration of carbon-12 with 7.1–20.1 MeV neutrons in dielectrics. *J Phys G Nucl Phys* 9:985–994
- Al-Najjar SAR, Abdel-Naby A, Durrani SA (1986) Fast-neutron spectrometry using the triple- α reaction in the CR-39 detector. *Nuclear Tracks* 12:611–615
- Antolković B, Dolenc Z (1975) The neutron-induced $^{12}\text{C}(n,n')3\alpha$ reaction at 14.4 MeV in a kinematically complete experiment. *Nuclear Phys A* 237:235–252
- Chien C-C, Hodko D, Minevski Z, Bockris JO'M (1992) On an electrode producing massive quantities of tritium and helium. *J Electroanal Chem* 338:189–212
- Durrani SA, Bull RK (1987) *Solid state nuclear track detection*. Pergamon, Oxford
- Frenje JA, Li CK, Séguin FH, Hicks DG, Kurebayashi S, Petrasso RD, Roberts S, Glebov VY, Meyerhofer DD, Sangster TC, Soures JM, Stoeckl C, Schmid GJ, Lerche RA (2002) Absolute measurements of neutron yields from DD and DT implosions at the OMEGA laser facility using CR-39 track detectors. *Rev Sci Instrum* 73:2597–2605
- Jones SE, Palmer EP, Czirr JB, Decker DL, Jensen GL, Thorne JM, Taylor SF, Rafelski J (1989) Observation of cold nuclear fusion in condensed matter. *Nature* 338:737–740

- Jones SE, Palmer EP, Czirr JB, Decker DL, Jensen GL, Thorne JM, Taylor SF, Rafelski J (1990) Anomalous nuclear reactions in condensed matter: recent results and open questions. *J Nucl Fus Energy* 9:199–208
- Lawsen JD (1957) Some criteria for a power producing thermonuclear reactor. *Proc Phys Soc B* 70:6–10
- Lipson AG, Lyakhov BF, Roussetski AS, Akimoto T, Mizuno T, Asami N, Shimada R, Miyashita S, Takahashi A (2000) Evidence for low-intensity D-D reactions as a result of exothermic deuterium desorption from Au/Pd/PdO:D heterostructure. *Fus Technol* 38:238–252
- Mizuno T, Akimoto T, Ohmori T, Takahashi A, Yamada H, Numata H (2001) Neutron evolution from a palladium electrode by alternate absorption treatment of deuterium and hydrogen. *Jpn J Appl Phys* 40:L989–L991
- Mosier-Boss PA, Szpak S, Gordon FE, Forsley LPG (2007) Use of CR-39 in Pd–D co-deposition experiments. *EPJ Appl Phys* 40:293–303
- Nikezic D, Yu KN (2004) Formation and growth of tracks in nuclear track materials. *Mater Sci Eng R* 46:51–123
- Oriani RA, Fisher JC (2002) Generation of nuclear tracks during electrolysis. *Jpn J Appl Phys* 41:6180–6183
- Packham NJC, Wolf KL, Kainthla RC, Bockris JO'M (1989) Production of tritium from D₂O electrolysis at a palladium cathode. *J Electroanal Chem* 270:451–458
- Pálfalvi JK, Szabó J, Akatov Y, Sajó-Bohus L, Eördögh I (2005) Cosmic ray studies on the ISS using SSNTD, BRADOS projects, 2001–2003. *Radiat Meas* 40:428–432
- Phillips TW, Petrasso RD, Cable MD, Sangster TC, Hicks DG, Séguin FH, Li CK, Soures JM (1998) Charged-particle spectroscopy: a new diagnostic for inertial fusion explosions. *Inertial Confinement Fusion* 8:109–115
- Phillips GW, Spann JE, Bogard JS, VoDinh T, Emfietzoglou D, Devine RT, Moscovitch M (2006) Neutron spectrometry using CR-39 track etch detectors. *Radiat Prot Dosim* 120:457–460
- Sajó-Bohus L, Pálfalvi JK, Akatov Y, Arevalo O, Greaves ED, Németh P, Palacios D, Szabó J, Eördögh I (2005) Neutron-induced complex reaction analysis with 3D nuclear track simulation. *Radiat Meas* 40:442–447
- Séguin FH, Frenje JA, Li CK, Hicks DG, Kurebayashi S, Rygg JR, Schwartz B-E, Petrasso RD, Roberts S, Soures JM, Meyerhofer DD, Sangster TC, Knauer JP, Sorce C, Glebov VY, Stoeckl C, Phillips TW, Leeper RJ, Fletcher K, Padalino S (2003) Spectrometry of charged particles from inertial-confinement-fusion plasmas. *Rev Sci Instrum* 74:975–995
- Srinivasan M (1991) Nuclear fusion in an atomic lattice: an update on the international status of cold fusion research. *Curr Sci* 60:417–439
- Szpak S, Mosier-Boss PA, Smith JJ (1996) On the behavior of the cathodically polarized Pd–D system: search for emanating radiation. *Phys Lett A* 210:382–390
- Szpak S, Mosier-Boss PA, Boss RD, Smith JJ (1998) On the behavior of the Pd–D system: evidence for tritium production. *Fus Technol* 34:38–51
- Szpak S, Mosier-Boss PA, Miles M, Fleischmann M (2004) Thermal behavior of polarized Pd–D electrodes prepared by co-deposition. *Thermochemica Acta* 410:101–107
- Szpak S, Mosier-Boss PA, Gordon FE (2007) Further evidence of nuclear reactions in the Pd–D lattice: emission of charged particles. *Naturwissenschaften* 94:511–514
- Takahashi A (1994) Some considerations of multibody fusion in metal-deuterides. *Trans Fus Technol* 26(4T):451
- Takahashi A, Takeuchi T, Iida T, Watanabe M (1990) Emission of 2.45 MeV and higher energy neutrons from D₂O–Pd cell under biased-pulse electrolysis. *J Nucl Sci Technol* 27:663–666
- Yoshioka T, Tsuruta T, Iwano H, Danhara T (2005) Spontaneous fission decay constant of ²³⁸U determined by SSNTD method using CR-39 and DAP plates. *Nucl Instr Meth Phys Res A* 555:386–395
- Ziegler JF, Biersack JP (1985) The stopping and range of ions in solids. Pergamon, New York

S1: ADDITIONAL DATA AND DISCUSSION

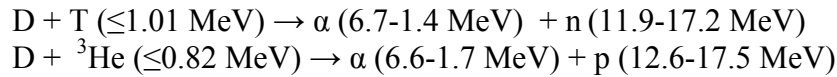
The primary reactions that occur in DD are (Séguin et al. 2003):



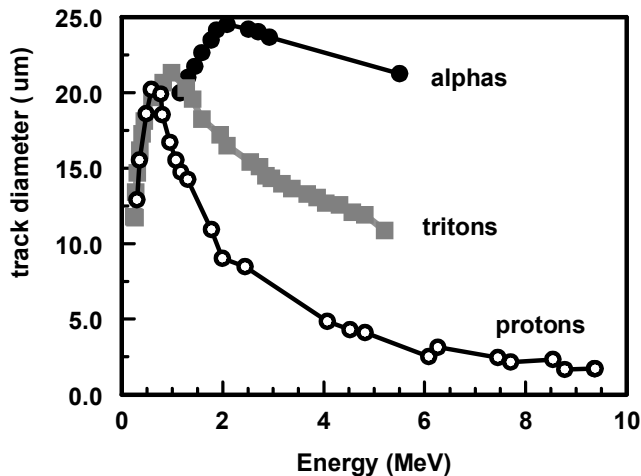
Since D_2O contains some T, the following reaction is also possible but only if the triton becomes slightly energetic ($\geq 8 \text{ keV}$):



Possible secondary reactions are:

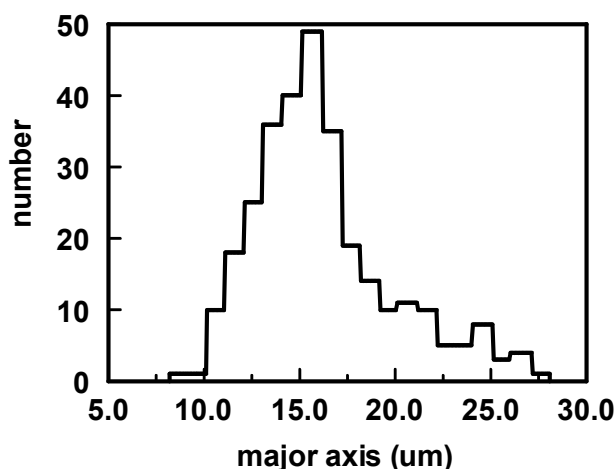


The protons, alphas, tritons, and ${}^3\text{He}$ formed in the primary DD reactions will leave tracks on the front surface of the CR-39 detector. The size of the pit created in the CR-39 detectors depends upon the size, energy, and charge of the particle that created the pit. Calibration curves have been generated by exposing CR-39 detectors to particles generated by an accelerator. One such calibration curve is shown in ESM-Figure 1. This



ESM-Figure 1. An example of a CR-39 calibration curve (adapted from data published in Séguin et al. 2003). CR-39 detectors were etched in 6.25 N NaOH at 80 °C for 6 hr. The CR-39 used was obtained from TASL.

calibration curve cannot be used to analyze our results as the etching conditions are different and our CR-39 was obtained from Fukuvi. It should be noted that there are variations in the quality of CR-39 between different manufacturers as well as batch-to-batch variation. To address this issue, we routinely expose one corner of our CR-39 detectors to an ${}^{241}\text{Am}$ source and use its alpha tracks as an internal standard. The calibration curves shown in ESM-Figure 1 were obtained under controlled conditions (either in a vacuum or in air) and imply that it would be relatively easy to differentiate between $> 1 \text{ MeV}$ protons, tritons, and alpha particles. However, as shown in ESM-Figure 2, the 5.5 MeV alpha particles emitted from an ${}^{241}\text{Am}$ source range in size from 10



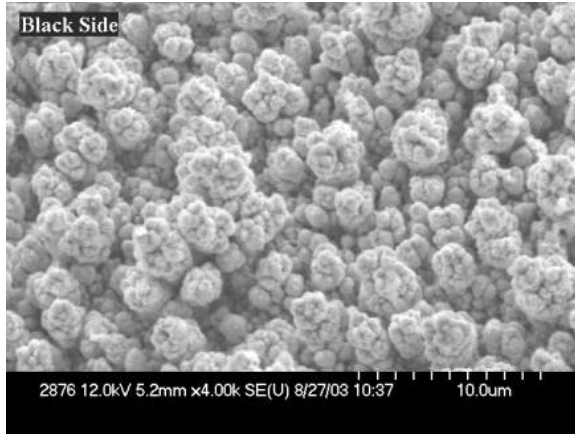
ESM-Figure 2. Size distribution of tracks obtained for CR-39 exposed to an ^{241}Am alpha source. Distance between the CR-39 detector and the ^{241}Am source is ~ 2 mm (our work).

to 25 microns. This size distribution is the result of scattering of the particles and is a function of the distance between the source and the CR-39 detector. The greater the distance between the source and the detector, the greater the energy loss and the more oblique the angle of incidence. Likewise the particles produced during Pd-D co-deposition will also exhibit a size distribution. In addition, speciation of the particles will be further complicated by the fact that the particles will have to traverse through a layer of water before they reach the CR-39 detector. The presence of water will slow the particles down resulting in a loss of energy. The decrease in energy can be determined using LET curves. ESM-Table 1 summarizes the decrease in energy of protons, tritons, helium-3, and alphas as a function of the thickness of the water layer:

ESM-Table 1. Decrease in the Energy of Protons, Tritons, ^3He , and Alphas as a Function of the Thickness of the Water Film Between the Source and the CR-39 Detector.

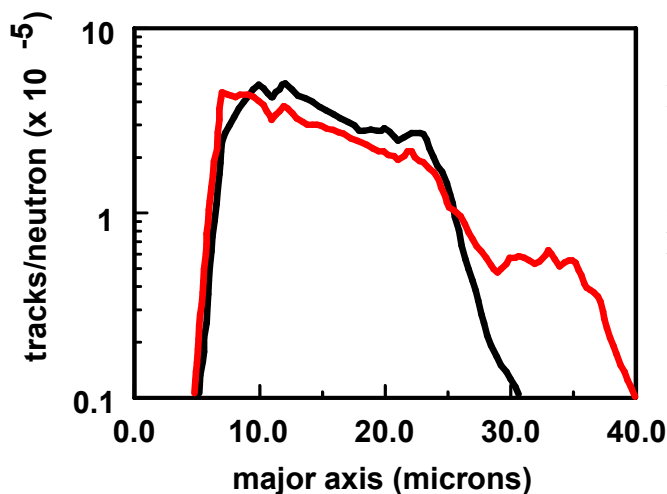
Thickness of Water Film (μm)	Decrease in Energy of Protons (MeV)	Decrease in Energy of Tritons (MeV)	Decrease in Energy of Helium-3 (MeV)	Decrease in Energy of Alphas (MeV)
1	0.07	0.04	0.08	0.08
2	0.15	0.10	0.25	0.23
3	0.22	0.18	0.45	0.45
4	0.28	0.26	0.70	0.65
5	0.33	0.35	0.90	0.90
10	0.52	0.7	1.75	1.85

ESM-Figure 3 shows an SEM of the Pd deposit formed as a result of Pd/D co-deposition. The Pd deposit is not smooth and has a cauliflower structure. Only particles formed near the surface of the deposit will have enough energy to traverse the water film and reach the CR-39. Because of the cauliflower structure of the Pd deposit, the thickness of the water film between the CR-39 detector and the Pd deposit will vary. The presence of a water layer will cause a shift to larger particle size in the size distribution. The variability in the thickness of the water layer will cause an increase in the range of particle sizes. Yet



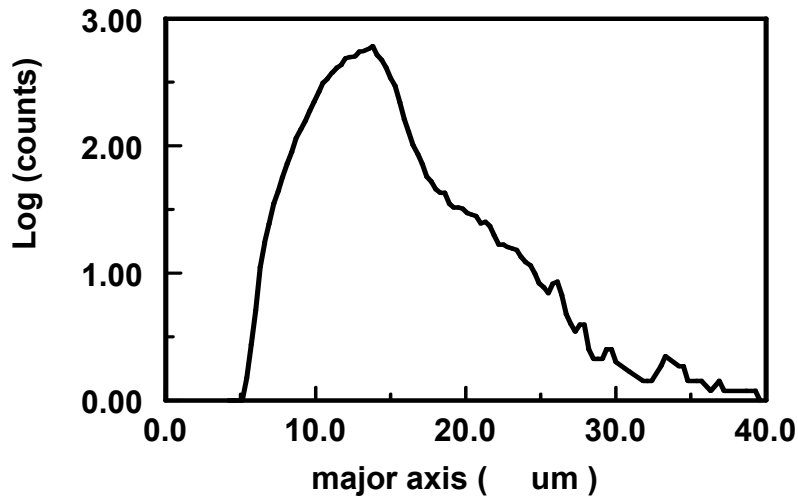
ESM-Figure 3. SEM of the Pd deposit formed as the result of Pd/D co-deposition (our work).

another complication is that neutron elastic interactions with CR-39 will leave latent recoil charged particle tracks (Phillips et al. 2006). The size distributions of the tracks formed by exposure to 2.5 and 14.8 MeV neutrons are shown in ESM-Figure 4. For the etching conditions used, the 2.5 MeV neutrons create tracks that range in size from 5 to 30 microns while the 14.8 MeV neutron tracks range is size between 5 and 40 microns. Consequently, if DD and DT fusion reactions are occurring in the Pd/D co-deposition experiments, the front side of the CR-39 detector in contact with the cathode will exhibit tracks resulting from collision with alphas, protons, tritons, ^3He , and neutrons. These particles will exhibit a larger than normal size distribution due to the presence of the water film. There will also be overlap between the size distributions of the various particles and the resultant size distribution will appear as a continuum (Mosier-Boss et al. 2007).



ESM-Figure 4. Track size distributions obtained on the front side of the CR-39 detector upon exposure to 2.5 MeV (black) and 14.8 MeV (red) monoenergetic neutrons (Phillips et al. 2006).

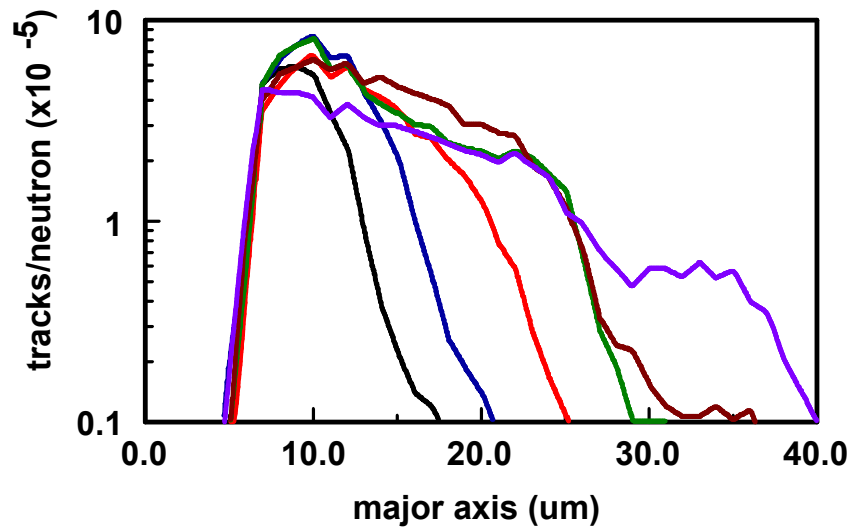
ESM-Figure 5 shows an example of the size distribution obtained on the backside of a CR-39 detector that has been used in a Pd/D co-deposition experiment. The LET curves indicate that the only charged particles that will traverse 1 mm thick CR-39 are >10 MeV protons, >43 MeV alphas, >17 MeV tritons, >33 MeV helium-3. Of the



ESM-Figure 5. Track size distribution obtained on the back side of a CR-39 detector that had been used in a Pd/D co-deposition experiment (our work).

primary and secondary reactions, only the 12.6-17.5 MeV protons will go through the CR-39, however, the pits will be very small. Neutrons will also go through the CR-39. The DD and DT neutrons can scatter elastically, producing recoil protons, carbons, or oxygen nuclei in the forward direction. But DT neutrons can also undergo two inelastic (n,p) and (n, α) reactions with carbon or oxygen. These inelastic reactions result in charged particles that can produce tracks on the front and/or the back side of the CR-39 detector. Given the size range of the tracks obtained for the backside of the CR-39, ESM-Figure 5, the tracks are indicative of neutrons and, unlike the front side, the size distribution on the backside of the CR-39 is not complicated by tracks due to alphas, protons, tritons, and helium-3.

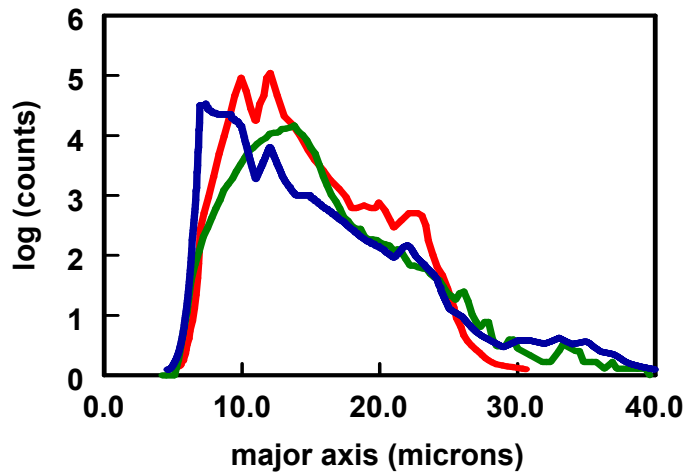
Phillips et al. (2006) have shown that neutron spectrometry can be done using CR-39. In their experiments, they exposed CR-39 detectors to monoenergetic neutrons. These monoenergetic neutrons are generated using two-body reactions such as DD, DT, ^7LiD , etc. Besides the primary neutrons, these reactions can produce additional particles such as protons, tritons, ^3He , and alphas. As discussed *vide supra*, while the energy of the protons formed as a result of the D- ^3He secondary reaction is sufficient to traverse the 1 mm thick CR-39 detector, the energies of the other charged particles are not. However, neutrons will go through the CR-39 and will undergo the elastic and inelastic reactions discussed above. These neutron-induced reactions will occur throughout the CR-39 detector. To differentiate the tracks due to the charged particles from the tracks resulting from the elastic and inelastic neutron reactions, the first 70 μm of the detector are etched away. After etching, the CR-39 detectors were analyzed using an automated system. The resultant size distribution for neutrons whose energies range from 0.144 to 14.8 MeV are shown in ESM-Figure 6. At low neutron energies, only recoil protons are seen and are observed as a peak at $\sim 10 \mu\text{m}$, ESM-Figure 6 0.144 MeV neutron. As the neutron energy increases, a broadening of the proton recoil peak at $\sim 10 \mu\text{m}$ is observed. At 1.2 MeV neutron energy, a second peak is visible at $\sim 25 \mu\text{m}$. This second peak is attributed to recoil carbon and oxygen atoms. For neutron energies between 1.2 and 8 MeV, the size



ESM-Figure 6. Track size distribution obtained on the front side of the CR-39 detector upon exposure to 0.114 MeV (black), 0.25 MeV (blue), 0.565 MeV (red), 1.2 MeV (green), 8 MeV (brown) and 14.8 MeV (purple) monoenergetic neutrons (Phillips et al. 2006).

distributions of tracks observed in the CR-39 detectors are roughly similar. In the CR-39 detector exposed to 14.8 MeV neutrons, a decrease in the proton recoil at $\sim 10 \mu\text{m}$ is observed, ESM-Figure 6, and a peak is observed at $\sim 35 \mu\text{m}$ which is attributed to the three alpha particle reactions. In the size distribution obtained for the CR-39 detector subjected to Pd/D co-deposition, ESM-Figure 5, there appears to be three populations of tracks. There is a fairly narrow peak at $\sim 12 \mu\text{m}$ which is attributed to recoil protons. A broader peak at $\sim 22 \mu\text{m}$ is observed that is assigned to recoil carbon and oxygen atoms. And there is a small peak at $\sim 33 \mu\text{m}$ attributed to the three alpha particle reactions, i.e., the carbon breakup reaction. These results are very preliminary and require additional analysis. However, it is interesting to note that in this particular analysis, there are ~ 25 tracks present between 30-40 μm , ESM-Figure 5. In our manual examinations of the CR-39 detectors, we identify at most 10 triple tracks that clearly show three particles breaking away from a center point. There are probably more in the regions of high track density. But for all intensive purposes there is agreement between the manual results and the scanned results.

ESM-Figure 7 shows a comparison of the track size distribution obtained on the backside of the CR-39 detector used in the Pd/D co-deposition reaction (ESM-Figure 5 multiplied by a factor of 1.5) with the track size distributions obtained for CR-39 detectors exposed to 2.45 and 14.8 MeV monoenergetic neutrons (Phillips et al. 2006). As discussed *vide supra*, DD fusion yields 2.45 MeV neutrons while DT fusion results in 14.8 MeV neutrons. The size distribution obtained as a result of Pd/D co-deposition exhibits features consistent with both DD and DT fusion. Both the CR-39 track size distributions obtained for DT fusion and Pd/D co-deposition show tracks between 30 and 40 microns that are attributable to the carbon breakup reaction. This peak is absent in the DD fusion track size distribution. Compared to DT fusion, the recoil proton peak observed for DD fusion is shifted to larger track size. The same is true of the recoil proton peak observed for CR-39 that has used in Pd/D co-deposition.



ESM-Figure 7. Comparison of track size distribution obtained on the back side of a CR-39 detector used in Pd/D co-deposition (green, our work) with CR-39 detectors that have been exposed to 2.45 (red, Phillips et al. 2006) and 14.8 (blue, Phillips et al. 2006) MeV neutrons

References

Mosier-Boss PA, Szpak S, Gordon FE, Forsley LPG (2007) Use of CR-39 in Pd/D co-deposition experiments. *EPJ Appl. Phys.* 40: 293-303.

Phillips GW, Spann JE, Bogard JS, VoDinh T, Emfietzoglou D, Devine RT, Moscovitch M (2006) Neutron spectrometry using CR-39 track etch detectors. *Radiat. Prot. Dosim.* 120: 457-460.

Séguin FH, Frenje JA, Li CK, Hicks DG, Kurebayashi S, Rygg JR, Schwartz B-E, Petrasso RD, Roberts S, Soures JM, Meyerhofer DD, Sangster TC, Knauer JP, Sorce C, Glebov VY, Stoeckl C, Phillips TW, Leeper RJ, Fletcher K, Padalino S (2003) Spectrometry of charged particles from inertial-confinement-fusion plasmas. *Rev Sci Instrum.* 74:975-995.